BrrICE1.1 is associated with putrescine synthesis through regulation of the arginine decarboxylase gene in freezing tolerance of turnip (Brassica rapa var. rapa)

Xin Yin(Former Corresponding Author)
Kunming Institute of Botany Chinese Academy of Sciences https://orcid.org/0000-0003-2664-2637
Yunqiang Yang
Kunming Institute of Botany Chinese Academy of Sciences
Yanqiu Lv
Chang Chun University
Yan Li
Kunming Institute of Botany Chinese Academy of Sciences
Danni Yang
Kunming Institute of Botany Chinese Academy of Sciences
Yanling Yue
Yunnan Agricultural University
Yongping Yang(New Corresponding Author) (yangyp@mail.kib.ac.cn)
https://orcid.org/0000-0002-0327-2664

Research article

Keywords: Brassica rapa var. rapa, freezing tolerance, transcriptome, metabolome, putrescine

Posted Date: March 30th, 2020

DOI: https://doi.org/10.21203/rs.3.rs-19586/v1

Version of Record: A version of this preprint was published on November 4th, 2020. See the published version at https://doi.org/10.1186/s12870-020-02697-6.

Abstract

Background: In the agricultural areas of Qinghai-Tibet Plateau, temperature varies widely from day to night during the growing season, which makes the extreme temperature become one of the limiting factors of crop yield. Turnip (Brassica rapa var. rapa) is a traditional crop of Tibet grown in the Tibet Plateau, but its molecular and metabolic mechanisms of freezing tolerance is unclear.

Results: Here, based on the changes in transcriptional and metabolic levels of Tibetan turnip under freezing treatment, the expression of the arginine decarboxylase gene BrrADC2.2 exhibited an accumulative pattern in accordance with putrescine content. Moreover, we demonstrated that the transcription factor BrrICE1.1 (Inducer of CBF Expression 1) could directly bind to the BrrADC2.2 promoter, activating BrrADC2.2 to promote the accumulation of putrescine, which was verified by RNAi and overexpression analyses for both BrrADC2.2 and BrrICE1.1 using transgenic hair root. The function of putrescine in turnip was further analyzed by exogenous application putrescine and its inhibitor DL-α-(Difluoromethyl) arginine (DFMA) under freezing tolerance. In addition, the BrrICE1.1 was found to be involved in the ICE1-CBF pathway to increase the freezing stress of turnip.

Conclusions: BrrICE1.1 could bind the promoter of BrrADC2.2 or CBFs to participate in freezing tolerance of turnip by transcriptomics and targeted metabolomics analyses. This study revealed the regulatory network of the freezing tolerance process in turnip and increase our understanding of the plateau crops response to extreme environments in Tibet.

Background

Polyamines are low molecular weight aliphatic polymers that are widely present in various organisms. Many types of polyamines, such as agmatine, putrescine, spermidine, spermine, and cadaverine, have been found in higher plants [1]. Among them, putrescine is the first key factor in polyamine metabolism in most organisms, and the synthesis of polyamines begins with the synthesis of putrescine. Putrescine in plants could be formed in two ways: one is mainly dependent on the arginine decarboxylase (ADC) pathway, and the expression of ADC mainly increases the accumulation of putrescine [2]. The other pathway involves direct catalysis by Orn decarboxylase (ODC) [3]. The ADC pathway is catalyzed by three enzymes in sequences: ADC, agmatine iminohydrolase (AIH), and N-carbamoylputrescine amidohydrolase (CPA). Additionally, spermidine and spermine were formed by sequential addition of aminopropyl groups to putrescine and spermidine, respectively, by spermidine synthase (SPDS) and spermine synthase (SPMS). The aminopropyl groups were generated from S-adenosylmethionine (SAM) by SAM decarboxylase [3].

Numerous studies have demonstrated that changes and balance in polyamine metabolism have important regulatory effects on the growth and stress response of many plants [4, 5], including that to chilling stress [6], high-temperature stress [7], drought [8], salinity [9], disease [10], and oxidative stress [11]. Increasing endogenous polyamines by genetic transformation of polyamine biosynthetic genes or

exogenous application of polyamines enhanced the tolerance in various plants [6, 12, 13]. For example, overexpression of the key genes ADC1 and ADC2 for putrescine synthesis in Arabidopsis thaliana increased the contents of putrescine, improving cold tolerance, but mutants defective in adc1 and adc2 displayed reduced freezing tolerance compared to control plants[8, 14]. Studies by Urano et al. also showed that ADC2 was induced under salt stress in Arabidopsis and that the content of free putrescine was regulated to enhance the resistance to stress, while the adc2 mutant was very sensitive to salt stress [9]. In addition, transgenic plants expressing the yeast SAMDC showed enhanced tolerance to high-temperature stress [15]. Additionally, exogenous polyamines and polyamine inhibitors are an important means to study the relationship between polyamines and plant stress resistance. For example, exogenous putrescine and spermidine could reduce the stress of salt-sensitive rice [16], but polyamine inhibitors (such as DFMA) reduced the cold tolerance of chilling-tolerant rice [17]. Furthermore, exogenous application of putrescine improved potato cold-acclimated freezing tolerance [6]. Therefore, regulation of the polyamine metabolic pathway is an effective way to improve plant resistance to stresses and has broad application prospects in plant breeding for stress resistance.

Freezing stress is a major factor that limits crop yield, preventing crop growth in millions of hectares worldwide and reducing the geographical distribution of crops. Plants have evolved complex mechanisms to adapt to extreme temperatures, such as low-temperature stress, which was accompanied by changes in the expression of thousands of genes [18]. Among them, the ICE1-DREB/CBF axis was identified as a key regulatory pathway under low temperature in plants [19]. ICE1 is a well-characterized helix-loop-helix (bHLH) protein that acts as an upstream regulator of the transcriptional regulation cascade of the cold response in Arabidopsis. ICE1 regulates the transcriptional expression of downstream genes by binding to the MYC element (CANNTG) on the promoter of the CBF gene, and CBF in turn regulates many cold-regulated (COR) genes [20–22]. However, the possibility of other unexplored potential mechanisms of ICE1 cannot be completely eliminated. In fact, in addition to the established ICE1-CBF cascade, the CdICE1 of chrysanthemum could also mediate freezing resistance by regulating the expression of the microRNA miR398 [23]. In particular, PtICE1 interacted with ADC, which is associated with the polyamine pathway regulating cold tolerance in Poncirus trifoliata [24]. Thus, some undetermined molecular mechanisms may also contribute to the cold tolerance of ICE1 and its homologues.

The Qinghai-Tibet Plateau has a special climate, with a high altitude, a low temperature, low oxygen, strong radiation, drought, strong wind and other adverse climatic conditions occurring frequently. In the long-term adaptation process, plants have evolved many survival strategies. In this regard, understanding how plants in Tibet adapt to and survive abiotic stresses is important for the efficient exploitation of genetic resources associated with desirable stress tolerance, for developing new approaches to enhance stress tolerance, and for providing important theoretical support for the analysis of multiple crops in the plateau. Turnip (Brassica rapa var. rapa) is a traditional crop in the Qinghai-Tibet Plateau that is used for food, feed and medicine and has good adaptability to the extreme environment in the long-term growth process of the Qinghai-Tibet Plateau [25]. Research has shown that Tibetan turnip was highly responsive to cold exposure [26]. However, very limited information was available about the mechanism underlying

the freezing tolerance of turnip. Analysis of the adaptability of turnip to the freezing environment will help elucidate the molecular mechanism of freezing tolerance of turnip and could also provide suggestions for breeding turnip in Tibet. In present study, through analysis of differential gene expression and weighted gene coexpression correlation network analysis (WGCNA) by transcriptome and metabonomic studies, we identified a key gene BrrADC2.2 that may be involved in putrescine metabolism. BrrICE1.1 binding to BrrADC2.2 promoter regulated putrescine synthesis which were identified by biochemical and Agrobacterium rhizogenes-mediated (LBA9402 strain) genetic transformation assays, indicating the important roles of putrescine in freezing stress tolerance. In addition to the classical ICE1-CBF-COR pathway, the polyamine metabolic pathway contributed to Tibetan turnip freezing resistance under extremely low temperature conditions.

Results

The Tibetan turnip KTRG-B49 response to freezing tolerance

We used the turnip KTRG-B49 variety from the Qinghai-Tibet Plateau to assess the freezing tolerance of turnip. As expected, compared with the control seedlings, most of the treated seedlings survived (Fig. 1A). With the extension of freezing stress time, the electrolyte leakage of the turnip cells increased gradually (Fig. 1B). When the plants were grown at -4 ℃ for 2 h, they displayed more serious damage than plants grown under standard conditions. After recovery growth for 12 h in an ambient environment, the plants were restored and had an electrolyte leakage of 23.9%, but there was still a high survival rate of 78.9% (Fig. 1C). These data indicated that KTRG-B49 had the reproductive characteristics of turnip on the Qinghai-Tibet Plateau and can respond to low temperatures.

Transcriptome changes in KTRG-B49 during freezing treatment

KTRG-B49 plants that underwent freezing treatment used for RNA-seq to determine the genes responsible for tolerance. Totals of 144.16 Gb clean data were obtained for 21 KTRG-B49 individuals, with more than 6.18 Gb for each sample. The sequencing quality scores of 30 (Q30) of the samples were greater than 89.03%, indicating the high quality of the reads (Table S2). Here, 83.27%-89.72% of the clean reads were mapped to the turnip reference genome using TopHat software with an average mapping rate of 86.56% (Table S3). Therefore, more than half of the turnip reference genes were expressed in each sample, which was sufficient for further differential gene expression analysis. A correlation analysis of the expression levels among the samples (Fig. S2) and the FPKM distribution for all samples (Fig. S3) showed that the repeatability of the expression level of each sample was good. In addition, the results of principal component analysis (PCA) based on the 21 samples showed that the first component explained 38.9% of the variation, and the second component explained 36% of the variation (Fig. 2A). KTRG-B49 could be clearly separated five distinct clusters along the first component axis. This finding indicated a close relationship between CK and C1 and between F2 and F4, which may have similar expression patterns. The differential expression analysis among different treatments can be inferred based on PCA.

The polyamine synthesis pathway is associated with the freezing responses of KTRG-B49

To investigate the gene expression levels, we calculated the FPKM values using the reads from RNA-seq. The number of differentially expressed genes (DEGs) and functional annotation information are shown in Fig. S4 and Table S4, respectively. In the analysis, the DEGs were statistically grouped into six subclusters based on their expression patterns in turnip at different treatment stages (Fig. S5). Interestingly, 347 genes in subcluster_1 demonstrated a similar trend in the PCA of the transcriptomic landscape, which deserves further study (Fig. 2B). Accordingly, KEGG enrichment analysis of the DEGs in subcluster_1 was conducted to identify pathways that played important roles in the freezing process. The top five pathways for the upregulated DEGs are displayed, and major pathways related to circadian rhythm-plant, plant-pathogen interaction, polyamine biosynthesis, and arginine (Fig. 2C), which could indicate their involvement in turnip freezing tolerance. Here, based on these results and the role of polyamine in freezing stress, we focused on the pathway of polyamine synthesis (Fig. 2D). The expression levels of the DEGs in the polyamine pathway were verified by qRT-PCR (Fig. 2E). Of these genes, *BrrADC1, BrrADC2.1*, *BrrADC2.2*, and *BrrAlH1.1* accumulated continuously under freezing stress, showing a similar trend to subcluster_1. These DEGs related to polyamine synthesis may play a special role in enhancing the freezing resistance in turnip.

Putrescine was specifically enriched in KTRG-B49 upon freezing treatment

To confirm that the polyamine pathway was associated with turnip freezing tolerance, we analyzed polyamine accumulation in KTRG-B49. The polyamine profiles were assessed with a focus on agmatine, putrescine, cadaverine, and spermidine. As shown in Fig. 3A, the contents of agmatine and spermidine remained almost unchanged during the freezing treatment when compared with those of the CK without freezing stress group. However, freezing treatment significantly increased the levels of putrescine, and its contents were especially high (25.34-32.27 nmol g-1 FW) compared with those of the CK group (24.98 nmol g-1 FW). Furthermore, the cadaverine levels were also significantly different from those of the CK group in the 12 h recovery stage after freezing treatment, although the contents were relatively low. Therefore, these specifically increased metabolites upon freezing treatment, especially putrescine, may be related to the freezing tolerance of KTRG-B49.

Gene correlation network analysis

First, the expression patterns of 3886 DEGs (FPKM $\geq$ 1) obtained from transcriptome sequencing were analyzed by WGCNA, and they were divided into three modules according to the similarity of their expression patterns (Fig. 3B). The numbers of unique genes in each module were 2378, 571, and 937 for the black, green, and turquoise colors, respectively. The gene expression profile of the entire module was obtained (Fig. S1). Then, the correlations between the modules and the traits were analyzed, and the data are shown in Fig. 3C. One module of interest was the turquoise module; the correlation coefficient of that module with putrescine was the highest (0.78, *P*-value = 0.00003), indicating that the module 'Turquoise' was closely related to putrescine accumulation in turnip. To further identify 'Turquoise' modular features, we used KEGG pathway analysis for deep analysis (Fig. S6). Six genes were included in the METurqoise module and were found to be involved in the 'arginine and proline metabolism' pathway (ko0330,

M00133). Among these genes, *BrrADC2.2* (GenBank number: MN630676) was found to participate in polyamine synthesis, and the increase in *BrrADC2.2* expression was consistent with the accumulation of putrescine under freezing treatment. Taken together, these results suggested that *BrrADC2.2* may play a key role in polyamine synthesis under freezing stress in turnip, and the upregulation of *BrrADC2.2* expression and the increase in putrescine could be essential for freezing tolerance of turnip.

Identification of upstream regulatory transcription factors of *BrrADC2.2*

We performed yeast one-hybrid assays to screen the transcription factors interacting with *BrrADC2.2* promoter as bait and the turnip cDNA library as prey, and positive colonies were partially sequenced and identified by BLAST analysis. Finally, we identified a cDNA of a *B. rapa* ICE1-like transcription factor and named it *BrrICE1.1* (GenBank number: MN630673) in our turnip. *BrrICE1.1* has the entire set of signature motifs required for defining a typical bHLH transcription factor (Fig. S7). In addition, ICE1 was reported to be able to bind specifically to the MYC recognition sequence (CANNTG). Thus, we further analyzed the promoter region of *BrrADC2.2* using the PlantCARE database (http://bioinformatics.psb.ugent.be/webtools/plantcare/html/). As expected, there was a potential MYC recognition element (CATTTG) (958-963) within the 1-kb region upstream of the ATG (Fig. 4A, Table S5). Therefore, we speculated that *BrrICE1.1* combined with the CATTTG element in the promoter region of *BrrADC2.2* plays a role in freezing tolerance. Moreover, we analyzed the promoter sequence of other DEGs in the polyamine pathway, and an additional six DEGs (*BrrADC1*, GenBank number: MN630674; *BrrADC2.1*, GenBank number: MN630675; *BrrAIH1.1*, GenBank number: MN630677; *BrrAIH1.2*, GenBank number: MN630678；*BrrSAMDC1.1*, GenBank number: MN630679；*BrrSPD2.1*, GenBank number: MN630681) were found to contain the MYC recognition element (Table S5).

BrrICE1.1 bound to the promoters of polyamine pathway DEGs in vitro and vivo

Possible interactions of *BrrICE1.1* with the MYC elements of the above gene promoters were tested using a yeast one-hybrid system. We found that *BrrICE1.1* could activate *BrrADC2.1pro::pAbAi*, *BrrADC2.2pro::pAbAi*, *BrrAIH1.1pro::pAbAi*, and *BrrAIH1.2pro::pAbAi*, but not their mutant, suggesting that the MYC elements, CATTTG sites for *BrrADC2.1* and *BrrADC2.2*, and CAATTG sites for the *BrrAIH1.1* and *BrrAIH1.2* promoters were necessary and required for *BrrICE1.1* binding (Fig. 4B) in yeast.

Next, using the well-established transient expression assay of *N. benthamiana* leaves, we further verified the transcriptional activation activity of BrrICE1 with above four genes (Fig. 4C). Coexpression of *35S::BrrICE1.1* with *BrrADC2.1pro::LUC, BrrADC2.2pro::LUC, BrrAIH1.1pro::LUC,* and *BrrAIH1.2pro::LUC* LUC could detect *LUC* activity, indicating that *BrrICE1* could to active their expression, respectively. Furthermore, ChIP experiments using *BrrICE1.1-6Flag* transgenic hair roots and an anti-Flag antibody were employed to confirm the binding of *BrrICE1.1* to these four gene promoters in vivo. qPCR revealed that only the *BrrICE1.1-6Flag* protein could immunoprecipitate the *BrrADC2.2* promoter region containing an element of CATTTG (compared to the IgG and WT) (Fig. 4D). Together, these data suggest that *BrrICE1.1* can directly bind to the promoter of *BrrADC2.2* and that the CATTTG elements presented in the *BrrADC2.2* promoter were the binding sites for *BrrICE1.1*.

Transgenic and RNAi hair roots showed altered levels of *BrrADC2.2* transcripts and polyamines

The effect of the *BrrADC2.2* gene on putrescine synthesis was further verified by using *A. rhizogenes*-mediated infection of the cotyledons of turnip to obtain *BrrADC2.2* transgenic and RNAi hairy roots (Fig. 5A). Fluorescence of the hairy roots overexpressing *BrrADC2.2-OE* was obtained by confocal laser microscopy (Fig. 5B). Moreover, we tested the expression levels of *BrrADC2.2* in *BrrADC2.2-OE* and *BrrADC2.2-RNAi* using qRT-PCR analysis (Fig. 5C). The expression of *BrrADC2.2* was significantly up- and down-regulated in *BrrADC2.2-OE* and *BrrADC2.2-RNAi* hair roots, respectively, compared with the control, indicating that the *BrrADC2.2* gene was successfully expressed in the roots. Additionally, the putrescine content of transgenic *BrrADC2.2-OE* measured by GC-MS was significantly higher than that of the control. As expected, *BrrADC2.2-RNAi* reduced the putrescine content (Fig. 5D). Both the *BrrADC2.2* expression levels and putrescine contents indicated that *BrrADC2.2* displayed a crucial role in putrescine synthesis.

BrrICE1.1 directly regulated *BrrADC2.2* in putrescine synthesis

To identify the role of *BrrICE1.1* in putrescine synthesis, we obtained transgenic and RNAi hairy roots (Fig. 5A). The *BrrICE1.1-GFP* fusion protein emitted a green fluorescent signal in the membranes and nuclei of the hair roots (Fig. 5A). Interestingly, cell membrane localization of *BrrICE1.1* was present in turnip but absent in *Arabidopsis* (Fig. 5E, left). To explore the membrane localization of turnip BrrICE1.1, we analyzed the protein structural characteristics of BrrICE1.1 and AtICE1.1 (Fig. 5F). We found that the C-terminus was conserved, while at the N-terminus, BrrICE1.1 had an extra signal peptide (GGGGERV). We speculated that this single peptide affected the location of BrrICE1.1. Hence, we deleted a single peptide of BrrICE1.1 in the turnip to test its location. We were surprised to find that its membrane localization disappeared and only nuclear localization was observed in *N. benthamiana* leaves (Fig. 5E, right). Therefore, this single peptide was indeed the reason for the localization of BrrICE1.1 in the membrane.

Efforts were further made to compare the expression levels and putrescine contents among transgenic, RNAi and WT hairy roots. The expression level of *BrrICE1.1* was slightly upregulated and *BrrADC2.2* was significantly upregulated in transgenic *BrrICE1.1-OE* hairy roots compared to WT roots, while the expression levels in BrrICE1.1-RNAi hairy roots were lower than those in the WT (Fig. 5G). With respect to putrescine contents, GC-MS measurement showed that transgenic lines increased the levels of putrescine, in contrast to a reduction in the RNAi hairy roots (Fig. 5H). The expression level analysis together with the putrescine content analysis presented here may indicate that *BrrICE1.1* positively regulates the expression of *BrrADC2.2* in freezing stress of turnip.

Effect of exogenous application of putrescine and its inhibitor on the freezing tolerance of turnip

To confirm the role of putrescine in freezing tolerance in turnip, exogenous putrescine and inhibitor were applied to the KTRG-B49 under freezing conditions, respectively (Fig. 6). There were no obvious changes in plant morphology between putrescine-treated, inhibitor-treated and control plants before application of the freezing treatments. When suffered to freezing treatment, the putrescine-treated plants suffered significant less injury compared with the control, whereas the inhibitor-treated plants the most severely

injured (Fig. 6A). To further confirm the results obtained above, electrolyte leakage was used to measure the plants after freezing treatment. Consistently, electrolyte leakage of putrescine-treated leaves exhibited a significantly lower electrolyte leakage after freezing treatment (Fig. 6B). These results suggested that putrescine could play an important role in turnip freezing tolerance.

The CBF signaling pathway was enhanced by freezing stress in KTRG-B49

CBF represents a well-documented pathway involved in plant cold responses. To clarify the possible signal transduction, we monitored the expression levels of *BrrICE1.1*, *BrrCBF3* and the downstream *BrrCOR15A* genes in turnip under freezing stress. We observed an elevation of all three genes, although significance was not observed in all periods of the freezing treatment (Fig. 7). Next, we asked whether *BrrICE1.1* regulated *BrrCBF3* using in vivo and in vitro methods. We first analyzed the promoter region of *BrrCBF3* and found that it contained the MYC recognition element (CATTTG) in a 1623 region (Fig. 8A), and thus, we confirmed that *BrrICE1.1* could bind to *BrrCBF3*. Indeed, Y1H assays revealed that *BrrICE1.1* could activate $BrrCBF3_{pro}$*::pAbAi*, suggesting that the *BrrICE1.1* binding sites may be CATTTG. The activation of *BrrICE1.1* on the reporters was completely abolished when CATTTG was deleted ($mBrrCBF3_{pro}$), suggesting that the CATTTG element in the *BrrCBF3* promoter was necessary and required for *BrrICE1.1* binding in yeast (Fig.7B). We thus performed LUC assays to determine the effect of *BrrICE1.1* on the expression of a reporter containing the *BrrCBF3* promoter fused with the LUC reporter gene. We found that coexpression of *35S::BrrICE1.1* with the *BrrCBF3pro::LUC* reporter led to an obvious increase in LUC activity, indicating that BrrICE1.1 activated the expression of *BrrCBF3* (Fig. 8C). To confirm this effect, we used ChIP-qPCR analysis. An IgG antibody and WT were used as controls, and two different sets of primers, *CBF3* promoter primers containing CATTTG elements (*BrrCBF3*) and *CBF3* gene background primers (*BrrCBF3-GD*), were used to test the *BrrICE1.1-6Flag* immunoprecipitated complexes. Notably, BrrCBF3 promoter primer enrichment was significantly increased in *BrrICE1.1-6Flag* immunoprecipitated complexes (Fig. 8D). This finding implied that *BrrICE1.1* directly regulated *BrrCBF3*. To examine the function of *BrrCBF3* and *BrrICE1.1*, we generated *BrrICE1.*1 overexpression and RNAi hair roots. Overexpression of *BrrICE1.1* led to enhanced induction of the *BrrCBF3* gene, whereas the expression level of *BrrCBF3* was downregulated in the BrrICE1.1-RNAi hair roots (Fig. 8E). These investigations suggested that the *BrrICE1.1* signal pathway could be associated with CBF-mediated freezing tolerance in turnip.

Discussion

Low temperature restricts the growth and geographical distribution of plants, and thus, major crop losses caused by low temperature injury are observed every year worldwide [27]. In the agricultural area of the Qinghai-Tibet Plateau, the average temperature of the crop growing season is very low, and extreme temperature has become one of the limiting factors of crop yield. Therefore, it is necessary to reveal the metabolism and molecular mechanisms of crops under freezing stress, which will help cultivate freezing-tolerant crop varieties, thereby reducing production losses. Tibetan turnip is suitable for cultivation in the alpine region due to its freezing resistance; this plant showed strong freezing tolerance and good

adaptability to the climate in Tibet [26]. In turnip, the pathways responding to freezing stress have not been systematically investigated. Analysis of the adaptability of turnip to a low-temperature environment will help elucidate the molecular mechanism of freezing tolerance of turnip and could also provide suggestions for breeding turnip in Tibet. In our study, we first showed that turnip KTRG-B49 could resist freezing tolerance and to some extent elucidated the characteristics of freezing resistance of turnip in Tibet (Fig. 1).

The increase in *BrrADC2.2* expression is consistent with the accumulation of putrescine under freezing treatment

Upon exposure to cold stress, the metabolic and physiological status of plants is altered, which is accompanied by changes in the expression of thousands of genes [18]. For example, polyamine has been suggested to be a crucial factor in the response of plants to low temperature [12, 24]. In the current study, expression profile analysis of differentially expressed genes (DEGs), which was similar to PCA analysis with a transcriptome background, showed enrichment in the polyamine pathway (Fig. 2A, 2B, 2C, Fig. S4). Furthermore, polyamines, particularly putrescine (Put), have been proposed to play an important role in the ability of plants to cope with cold stress. In our study, free putrescine continued to accumulate rapidly and specifically under low-temperature stress, reaching a high level (Fig. 3A). In addition, the content of polyamines in plants can be used as an important index to measure their resistance to stress, as polyamine-rich plants usually show high resistance to stress [9, 13, 28, 29]. However, no noteworthy changes were found in the agmatine and spermidine contents. Similar results indicated that putrescine's downstream product spermidine did not increase with putrescine content [6], and another study reported that the putrescine content of *A. thaliana* and *Thellungiella halophila* was improved, but its precursors showed no significant variation under cold treatment [30]. It was thus suggested in our study that the specific increase in the putrescine content may be closely related to the stress signal in response to low-temperature stress and may slow the damage due to low temperatures and enhance the freezing resistance in turnip.

The polyamine pathway is complex and involves many key enzymes [1, 6], including putrescine, which was synthesized in one step by ODC or in three steps by ADC, AIH and CPA [2, 3]. Our WGCNA revealed that the expression of *BrrADC2.2* showed accumulation along with the putrescine contents, indicating that *BrrADC2.2* was involved in the synthesis of endogenous putrescine under freezing treatment in turnip (Fig. 3B, 3C). In *Arabidopsis*, overexpression of the *ADC2* gene increased the freezing tolerance of transgenic plants [31, 32] and *adc2* mutants could restore freezing tolerance to wild-type levels by exogenous putrescine application [14]. Interestingly, induction of *ADC2* was also associated with osmotic stress, wounding, light, sucrose, flower development, seed germination, and salinity [31-35]. Thus, *BrrADC2.2*-catalyzed putrescine synthesis may promote the freezing tolerance of turnip, and these results provide useful information for further research on the molecular mechanism by which *BrrADC2.2* participates in freezing tolerance in turnip.

BrrICE1.1 directly binding to the *BrrADC2.2* promoter regulates the synthesis of putrescine

At present, there are few studies on the regulatory relationship between the *ADC* and other genes. Prior research only pointed out that the *ADC1*-associated putrescine pathway plays an important role in the cold-acclimated freezing tolerance of potatoes, most likely by enhancing the expression of CBF genes [6]. Furthermore, the *ADC* interaction with *PtrICE1* was only verified by a yeast two-hybrid assay and shown to modulate the polyamine levels that may be involved in cold tolerance [24]. In the current study, *BrrADC2.2* was activated by *BrrICE1.1* of turnip, as shown through in vivo and in vitro assays, which were crucial in deciphering the freezing signaling pathway related to freezing tolerance and identifying valuable gene candidates for genetic manipulation (Fig. 4). Additionally, previous studies have noted that *ICE1* regulates target genes through binding to the MYC (CANNTG) element in the promoter region functioning in cold signaling [20]. To the best of our knowledge, binding between the *BrrADC2.2* promoter element (CATTTG) and the *BrrICE1.1* gene has not previously been described. Moreover, *ICE1* is a central regulator of the plant cold response [20, 36, 37]. The up- and down regulation of the expression level and putrescine level, respectively, in *BrrADC2.2* and *BrrICE1.1* transgenic and RNAi roots indicated that *BrrADC2.2* and *BrrICE1.1* were involved in the synthesis of putrescine in turnip (Fig. 5). Thus, our data demonstrated that *BrrICE1.1* played a positive role in putrescine synthesis, likely in response to freezing tolerance through binding to *the BrrADC2.2* promoter. Foliar applied putrescine due to their ability to act as growth regulator is able to modulate the plant metabolism and the production of metabolites involved in stress tolerance [6]. In our research, both the exogenous application of putrescine and its inhibitor further confirmed the function of putrescine under freezing tolerance in turnip (Fig. 6).

The reason of the cell membrane localization of the BrrICE1.1 protein

Notably, the GFP-BrrICE1.1 fusion protein was located in the cell membrane and nucleus in our study (Fig. 5E, 5F), in contrast to the nuclear localization of GFP-AtICE1 in *Arabidopsis* [20]. By deleting the N-terminal extra single peptide (GGGGERV) of the BrrICE1.1 protein compared with AtICE1, the membrane localization of the BrrICE1.1 protein disappeared, suggesting that this single peptide affected the location of the BrrICE1.1 protein. This membrane-associated NAC transcription factor, similar to NAC089, ensured rapid transcriptional responses to incoming stimuli in *Arabidopsis* and could relocate from the ER membrane to the nucleus under ER stress conditions [38, 39]. The cell localization disparity between *BrrICE1.1* and AtICE1 in response to freezing might be presumably ascribed to the different cell location in the plant species, which is an important issue for future research. These findings provide new knowledge of the function and underlying mechanism of ICE1 and expand our understanding of the complex cold signaling network.

BrrICE1.1-BrrCBF3 pathway is involved in the freezing stress of the turnip

Here, we could not eliminate the contribution of other signaling pathways besides the putrescine pathway to the freezing tolerance of turnip, so we attempted to link it with known freezing stress-related signaling pathways. The CBF regulatory pathway is known to be one of the most important pathways and plays a key role in cold signal transduction in many species [20, 37, 40, 41]. In current study, freezing stress led to enhanced induction of CBF3 and the downstream COR genes (Fig. 7). Moreover, *BrrICE1.1* was shown to

bind to the promoters of *BrrCBF3* at CATTTG sites (Fig. 8A, B, C, D). This finding was similar in *Arabidopsis* because the *ICE1* gene could bind directly to the canonical *MYC cis*-elements (CANNTG) in the *CBF3* promoter [20]. Additionally, changes in the *BrrCBF3* expression patterns were consistent with those in the hair roots with overexpression and silencing of *BrrICE1.1* (Fig. 8E), implying that *BrrICE1.1* played a positive role in *BrrCBF3*-mediated freezing signaling in turnip.

Conclusions

Based on the results obtained in this study that transcriptomics and targeted metabolomics analyses provided new insights into freezing tolerance in Tibetan turnip, a working model of the BrrICE1.1 regulatory network involved in the turnip freezing process was proposed (Fig. 8F). The above-mentioned illustration suggested that modulation of cellular polyamine content could be regarded as a convenient and effective strategy to enhance freezing tolerance.

Methods

Plant cultivation, freezing treatment and electrolyte leakage measurement

Seeds of *Brassica rapa* var*. rapa* (KTRG-B49) were obtained from the Germplasm Bank of Wild Species, Kunming Institute of Botany, Chinese Academy of Sciences, Kunming, China, which were collected from Basu County, Changdu District, Tibet, China (N30°03'25.76"□E96°55'37.70"). The harvested seeds were sown in a seedling-raising plate with appropriate watering under controlled greenhouse conditions (12 h light/12 h dark cycle; 28 °C day/25 °C night, 200 mmol photons $m^{-2}s^{-1}$ light intensity, relative humidity of 75-80%) at Kunming Institute of Botany. For freezing treatment, 2-week-old plants (approximately 100 seedlings in each experiment) were assayed as described [42]. Briefly, the plants were incubated at 4 °C for 6 h. Then, the temperature was successively decreased by 2 °C h^{-1} until reaching -2 °C and was held at -2 °C for 2 h and -4 °C for 1 h in a programmed incubator. Next, the plants were kept overnight at 4 °C for 12 h and then returned to the greenhouse conditions for recovery, followed by an assessment of the survival rate. In the meanwhile, untreated plants were used as control, and other conditions were unchanged. Leaf-samples (randomization approach) were collected from the plants after freezing treatment for 0 h (CK), 4 °C for 1 h (C1), 3 h (C4), 6 h (C6), -2 °C for 2 h (F2), -4 °C for 1 h (F4) and recovery for 12 h (R12), then immediately frozen in liquid nitrogen and then stored at - 80 °C. Collection was performed from more than 3 plants at each sampling time, and each sample collection was repeated 3 times to obtain biological replicates (the three biological replicates included three separate set of freezing stress treatment experiments). There were 21 samples in total used for RNA-seq and metabolite analysis. Also, the electrolyte leakage was used to evaluate freezing tolerance at each sampling time following the previously described method [43].

Illumina RNA-sequencing and data analysis

Total RNA was isolated from 21 leaf-samples and messenger RNA (mRNA) was purified and used to generate short fragments via fragmentation buffer. Next, a random hexamer primer was used to synthesize the first-strand cDNA using these mRNA fragments as templates, and the second strand was synthesized using dNTPs, RNase H and DNA polymerase I. The fragments were retrieved and connected with sequencing adapters. Finally, the fragments were selected using agarose gel electrophoresis separation and enriched by PCR amplification. The library was paired-end 100-bp sequenced using an Illumina HiSeq 2000 system. The RNA-seq raw sequence data reported in this paper have been deposited in the Genome Sequence Archive in BIG Data Center [44] under accession numbers CRA001940 that are publicly accessible at https://bigd.big.ac.cn/gsa.

Clean reads were obtained by removing unacceptable reads, such as adapters and unknown ('N' > 5%) and low-quality bases (scores < 20), from the raw reads. The clean reads were then mapped to the turnip reference genome [45] with the TopHat 2.0.8 program [46]. FPKM (fragments per kilobase of exon per million mapped reads) was used to estimate gene expression levels by Cufflinks normalization (http://cufflinks.cbcb.umd.edu/), and differential expression analysis was performed using the DESeq R package (1.10.1) [47]. A false discovery rate (FDR) ≤ 0.001 and fold change ≥ 4 were used as the threshold to judge the significance of gene expression differences (DEG). Sequences were aligned against protein databases using BLASTx, including the NCBI non-redundant protein (Nr), Swiss-Prot, KEGG (http://www.genome.jp/kegg/kegg2.html), and GO (http://wego.genomics.org.cn/cgi-bin/wego/index.pl) databases by a cutoff e-value of 10^{-5}.

RNA extraction, quantitative real-time PCR (qRT-PCR)

Total RNA was extracted for each sample using the Eastep® Super Total RNA Extraction Kit (Promega, Madison, WI, USA). Then, approximately 5 μg of RNA was reverse transcribed to generate cDNA using the GoScript Reverse Transcription System (Promega, Madison, WI) to generate cDNA. qRT-PCR was conducted in triplicate with different cDNAs synthesized from different treatments using FastStart Universal SYBR Green Master (Rox, Roche, Indianapolis, IN, USA) and a 7500 Sequence Detection System (Applied Biosystems, USA). The reaction parameters for thermal cycling were as follows: 95 °C for 10 min, followed by 40 cycles of 94 °C for 5 s and 60 °C for 15 s. *B. rapa* tubulin beta-2 chain-like (LOC103873913) was amplified as an internal control [25]. The primers used for qRT-PCR are listed in Table S1. Statistical analysis was performed using the software IBM SPSS Statistics 20.0.

Metabolite extraction and derivatization

An aliquot of each individual sample was precisely weighed and transferred to a centrifugal tube. After the addition of 500 μL of extract solvent (precooled at -20 °C, acetonitrile-methanol-water, 2:2:1), the samples were vortexed for 30 s, homogenized at 45 Hz for 4 min, and sonicated for 5 min in an ice-water bath. The homogenate and sonication cycle were repeated 3 times, followed by incubation at -20 °C for 1 h and centrifugation at 12000 rpm at 4 °C for 15 min. Then, 200 μL of supernatant was used for LC-MS analysis. For UHPLC-MS/MS analysis, a 100 μL aliquot of the clear supernatant (or standard solution)

was further transferred to a centrifugal tube and then mixed with 50 µL of 20 mg/mL dansyl chloride in acetone and 50 µL of 0.1 mol/L sodium carbonate after 60 min incubation at 40 °C in the dark. Dansyl derivatives were added to 50 µL of 1% formic acid in water, and the samples were vortexed for 30 s and centrifuged at 12000 rpm and 4 °C for 15 min. An 80 µL aliquot of the clear supernatant was transferred to an autosampler vial for UHPLC-MS/MS analysis.

Weighted gene coexpression network analysis (WGCNA)

WGCNA was performed using the R package (version 3.4.1) to construct a gene coexpression network. The genes with FPKM values > 1 used for the network were based on the above RNA-seq data from 7 samples of different freezing treatments, using each biological and technical replicate as an individual dataset (for a total of 21 samples). A topological overlap matrix was constructed with a threshold power of 10 (Fig. S1), and the TOM similarity algorithm was used to transform the adjacency matrix into a topological overlap matrix to reduce noise and false correlation. A dynamic tree cut procedure (mergeCutHeight = 0.25, minModuleSize = 30) was performed to identify similar modules in a hierarchal clustering tree. Modules were defined as branches of the dendrogram obtained from clustering and labeled by colors beneath the dendrogram. The first principal component of each module was defined as the module eigengene (ME), which could be considered a weighted average of the gene expression profiles that made up the module. The module membership was defined as the correlation of the expression profile and each ME. To discover any significant relationships between gene expression perturbations within modules and traits, we computed the correlations between MEs and stress stimulations. A *P*-value < 0.05 was considered to indicate a significant correlation between the module and the trait.

Yeast one-hybrid (Y1H) screening

The Y1H experiment was conducted using the Matchmaker^{TM} Gold Yeast One-Hybrid Library Screening System (Clontech) according to the manufacturer. The promoter region (2000 bp upstream from the initiation codon) of *BrrADC2.2* was cloned into the pAbAi vector as bait and transformed into Y1HGold. The antibiotic resistance was tested on SD medium lacking Ura in the presence of aureobasidin A (SD/Ura+AbA). Then, a cDNA pool of turnip and a SmaI-linearized pGADT7-RecAD cloning vector were cotransformed into the Y1HGold strain that had been created. Positive clones were screened by yeast colony PCR, and the PCR products were then analyzed by sequencing.

For the yeast one-hybrid validation assays, the promoters of *BrrADC1*, *BrrADC2.1*, *BrrADC2.2*, *BrrAIH1.1*, *BrrAIH1.2, BrrSAMDC1.1*, and *BrrSPD2.1* were also separately cloned into the pAbAi vector, and the CDS of *BrrICE1.1* was subcloned into the pGADT7 vector. For generation of these promoters with mutations, site-directed mutagenesis was used to delete the CANNTG motif of these promoters using the TaKaRa MutanBEST kit. Yeast one-hybrid assays were carried out using the Frozen-EZ Yeast Transformation II Kit (Zymo Research, Irvine, CA, USA). The antibiotic resistance was tested on SD medium lacking Ura in the

presence of aureobasidin A (SD/Ura+AbA). The DNA-protein interaction was selected on SD (-Ura /Leu+AbA) medium. The primers used in this study are listed in Table S1.

Transient expression assays in *Nicotiana benthamiana* leaves

The *luciferase* gene (*LUC*) sequence was recombined into the empty vector *PRI101-AN-Flag*, and the positive control plasmid *35s::luciferase-6Flag* was obtained. The *BrrADC2.1pro::LUC, BrrADC2.2 pro::LUC, BrrAlH1.1pro::LUC,* and *BrrAlH1.2pro:LUC* reporter constructs were generated using an approximately 2000 bp promoter sequence fused with the *LUC* reporter gene using the HindIII and SalI sites of the pRI101-AN DNA vector. All primers used in this experiment are listed in Table S1. A similar approach was used to generate the *35S::BrrICE1.1-6Flag* construct. The *35S::BrrICE1.1-6Flag* plasmids were coinfiltrated with the *pro::LUC* reporter gene into *N. benthamiana* leaves using the *A. tumefaciens* EHA105 strain, as described previously. Infiltrated plants were incubated at 22 °C for 72 h. Then, a Tanon 5200 automatic chemiluminescence image analysis system (Tanon, Shanghai, China) was used to capture LUC images and determine the luminescence intensity. Leaves were sprayed with 100 mM luciferin and placed in the dark for 3 min prior to luminescence detection. At least five independent LUC quantifications were assessed, with similar results.

A. rhizogenes-mediated transformation

The CDSs of *BrrICE1.1* and *BrrADC2.2* and their reverse complementary sequences were cloned into *PRI101-AN-Flag* vectors. Then, these constructs were separately transferred into *A. rhizogenes* LBA9402 by electroporation [48]. Cotyledon infection was used to transform the above genes into turnip roots, and the gene expression levels and putrescine content in the hair roots were extracted and analyzed by qRT-PCR and LC-MS, respectively, as described above. The transgenic hair roots of *BrrICE1.1-6Flag* were also used for chromatin immunoprecipitation (ChIP) assays. The primers used in this study are listed in Table S1.

ChIP assay

The ChIP experiment was carried out as described with minor modifications [49]. Briefly, 2 g of *BrrICE1.1-6Flag* transgenic hairy roots and empty *6Flag* vector (WT) hairy roots were crosslinked in 1% formaldehyde buffer. The fixed roots were extracted and washed to purify the nuclei. The nuclei were suspended in nuclei lysis buffer, and the chromatin solution was sonicated to shear the DNA (kept on ice, sonication time 30 s, interval time 30 s, 30 times, power 400 w, JY92-2). A sonicated mixture (SDS concentration = 0.1%) was added to ChIP dilution buffer and incubated with DYKDDDDK Tag (D6W5B) rabbit mAb (Bibds to same epitope as Sigma's Anti-FLAG M2® Antibody) and negative control antibody lgG. The protein-DNA complexes were collected by incubation with equilibrated Protein A+G Magnetic beads (LOT: 2923270). Then, the bead-protein-DNA complexes were washed and protein-DNA complexes were released by incubation with ChIP elution buffer. Then, 5 M NaCl was used to reverse the crosslinking. After the immunoprecipitated DNA was purified, qPCR was conducted to measure the

BrrADC2.1/BrrADC2.2/BrrAIH1.1/BrrAIH1.2 promoter fragment levels. Gene body (GD) primers were also used as a control. The primers used are shown in Table S1.

Subcellular localization

Subcellular localization assays were conducted in tobacco (*N. benthamiana*) leaves. The coding regions (CDS) of *BrrICE1.1* and *BrrICE1-m* (deletion of a single peptide) were cloned and fused into the binary vector PRI101-AN DNA with a green fluorescent protein (GFP) and were driven by the Cauliflower mosaic virus (CaMV) 35S promoter, forming a *35S:CDS*-GFP construct (the primers used are listed in Table S1). *A. tumefaciens* EHA105 carrying the construct of interest was infiltrated into *N. benthamiana* leaves. Fluorescence images were obtained under a laser-scanning confocal microscope (Olympus Optical Co., Ltd., Tokyo, Japan). GFP was excited with a 488-nm laser line, and emissions were captured using a 505-530 bandpass filter.

Application of exogenous putrescine and its inhibitor DL-α-(Difluoromethyl) arginine (DFMA)

Exogenous putrescine and its inhibitor (DFMA) were applied to the KTRG-B49 under freezing conditions, respectively, to test the effects of putrescine on potato freezing tolerance. The experiments were conduced referring to Yin *et al*. (2018). The 2-week-old plants were were sprayed with 1.5 mM putrescine and 0.5 mM DFMA once a day for 3 days, respectively, water was used in the control. The solutions were all supplemented with 0.01% (v/v) Tween 20 as a detergent. The plants were incubated at 4 °C for 6 h. Then, the temperature was successively decreased by 2 °C h^{-1} until reaching -2 °C and was held at -2 °C for 2 h, -4 °C for 1 h and -6 °C for 2 h in a programmed incubator. Next, the plants were kept overnight at 4 °C for 12 h and then leaves were used for the mearment of lectrolyte leakage.

Abbreviations

BrrICE1.1:Inducer of CBF expression 1; BrrCBF:C-repeat binding factor; BrrADC2.2:Arginine decarboxylase gene; COR:Cold-regulated; ADC:Arginine decarboxylase; ODC:Orn decarboxylase; AIH:Agmatine iminohydrolase; CPA:N-carbamoylputrescine amidohydrolase; SPDS:Spermidine synthase; SPMS:spermine synthase; SAM:S-adenosylmethionine; DFMA:DL-α-(Difluoromethyl) arginine; RNA:Ribonucleic acid; cDNA:Complementary deoxyribonucleic acid; RNA-seq:Ribonucleic acid sequencing; FPKM:Fragments per kilobase of exon per million mapped reads; PCA:Principal component analysis; DEGs:Differentially expressed genes; KEGG:Kyoto encyclopedia of genes and genomes; qRT-PCR:Quantitativereal-time PCR; WGCNA:Weighted gene coexpression correlation network analysis; bp:Base pair

Declarations

Ethics approval and consent to participate

Not applicable.

Consent for publication

Not applicable.

Availability of data and materials

The data sets generated or analyzed during this study were included in this published article and its additional files. All the transcriptome data from 21 samples have been deposited in the Genome Sequence Archive in BIG Data Center under accession numbers CRA001940 that are publicly accessible at https://bigd.big.ac.cn/gsa.

Competing interests

The authors declare that they have no competing interests.

Funding

This research was supported by the Strategic Priority Research Program of the Chinese Academy of Sciences, Pan-Third Pole Environment Study for a Green Silk Road (Pan-TPE) (Grant No. XDA2004010306), the Major Program of National Natural Science Foundation of China (31590820, 31590823), the National Natural Science Foundation of China (31601999 and 41771123), the West Light Foundation of the Chinese Academy of Sciences (to YQY), and the 13th Five-year Informatization Plan of Chinese Academy of Sciences□Grant No. XXH13506. The funders had no role in the design of the study and collection, analysis, and interpretation of data and in writing the manuscript.

Authors' contributions

Designed the experiments: YQY, YPY and XY. Performed the experiments: XY, YLV, and YLI, DY. Analyzed the data: YQY and XY. Contributed reagents/materials/analysis tools: XY, YQY, YLY. Wrote the paper: XY. All Authors read and approved the manuscript.

Acknowledgements

The authors thank all the student members of the laboratory for their technical assistance.

References

1. Gupta K, Dey A, Gupta B: **Plant polyamines in abiotic stress responses**. *Acta physiologiae plantarum* 2013, **35**(7):2015-2036.
2. Alcázar R, Marco F, Cuevas JC, Patron M, Ferrando A, Carrasco P, Tiburcio AF, Altabella T: **Involvement of polyamines in plant response to abiotic stress**. *Biotechnology letters* 2006, **28**(23):1867-1876.

3. Tiburcio AF, Altabella T, Borrell A, Masgrau C: **Polyamine metabolism and its regulation**. *Physiologia Plantarum* 1997, **100**(3):664-674.
4. Valero D, Martínez-Romero D, Serrano Ma: **The role of polyamines in the improvement of the shelf life of fruit**. *Trends in Food Science & Technology* 2002, **13**(6-7):228-234.
5. Bouchereau A, Aziz A, Larher F, Martin-Tanguy J: **Polyamines and environmental challenges: recent development**. *Plant science* 1999, **140**(2):103-125.
6. Kou S, Chen L, Tu W, Scossa F, Wang Y, Liu J, Fernie AR, Song B, Xie C: **The arginine decarboxylase gene *ADC1*, associated to the putrescine pathway, plays an important role in potato cold-acclimated freezing tolerance as revealed by transcriptome and metabolome analyses**. *Plant J* 2018, **96**(6):1283-1298.
7. Murkowski A: **Heat stress and spermidine: effect on chlorophyll fluorescence in tomato plants**. *Biologia plantarum* 2001, **44**(1):53-57.
8. Alcázar R, Cuevas JC, Patron M, Altabella T, Tiburcio AF: **Abscisic acid modulates polyamine metabolism under water stress in *Arabidopsis thaliana***. *Physiologia Plantarum* 2006, **128**(3):448-455.
9. Urano K, Yoshiba Y, Nanjo T, Igarashi Y, Seki M, Sekiguchi F, Yamaguchi-Shinozaki K, Shinozaki K: **Characterization of Arabidopsis genes involved in biosynthesis of polyamines in abiotic stress responses and developmental stages**. *Plant, Cell & Environment* 2003, **26**(11):1917-1926.
10. Witzell J, Kuusela T, Sarjala T: **Polyamine profiles of healthy and parasite-infected *Vaccinium myrtillus* plants under nitrogen enrichment**. *Journal of chemical ecology* 2005, **31**(3):561-575.
11. Rider J, Hacker A, Mackintosh C, Pegg A, Woster P, Casero RA: **Spermine and spermidine mediate protection against oxidative damage caused by hydrogen peroxide**. *Amino acids* 2007, **33**(2):231-240.
12. Palma F, Carvajal F, Ramos JM, Jamilena M, Garrido D: **Effect of putrescine application on maintenance of zucchini fruit quality during cold storage: Contribution of GABA shunt and other related nitrogen metabolites**. *Postharvest Biology and Technology* 2015, **99**:131-140.
13. Kasukabe Y, He L, Nada K, Misawa S, Ihara I, Tachibana S: **Overexpression of spermidine synthase enhances tolerance to multiple environmental stresses and up-regulates the expression of various stress-regulated genes in transgenic *Arabidopsis thaliana***. *Plant and Cell Physiology* 2004, **45**(6):712-722.
14. Cuevas JC, López-Cobollo R, Alcázar R, Zarza X, Koncz C, Altabella T, Salinas J, Tiburcio AF, Ferrando A: **Putrescine is involved in Arabidopsis freezing tolerance and cold acclimation by regulating abscisic acid levels in response to low temperature**. *Plant physiology* 2008, **148**(2):1094-1105.
15. Cheng L, Zou Y, Ding S, Zhang J, Yu X, Cao J, Lu G: **Polyamine accumulation in transgenic tomato enhances the tolerance to high temperature stress**. *Journal of Integrative Plant Biology* 2009, **51**(5):489-499.
16. Ndayiragije A, Lutts S: **Long term exogenous putrescine application improves grain yield of a salt-sensitive rice cultivar exposed to NaCl**. *Plant and soil* 2007, **291**(1-2):225-238.

17. Lee T-M, Lur H-S, Chu C: **Role of abscisic acid in chilling tolerance of rice (*Oryza sativa L.*) seedlings.: II. Modulation of free polyamine levels**. *Plant Science* 1997, **126**(1):1-10.
18. Chinnusamy V, Zhu J, Zhu J-K: **Cold stress regulation of gene expression in plants**. *Trends in plant science* 2007, **12**(10):444-451.
19. Guo X, Liu D, Chong K: **Cold signaling in plants: Insights into mechanisms and regulation**. *J Integr Plant Biol* 2018, **60**(9):745-756.
20. Chinnusamy V, Ohta M, Kanrar S, Lee B-h, Hong X, Agarwal M, Zhu J-K: **ICE1: a regulator of cold-induced transcriptome and freezing tolerance in *Arabidopsis***. *Genes & development* 2003, **17**(8):1043-1054.
21. Toledo-Ortiz G, Huq E, Quail PH: **The Arabidopsis basic/helix-loop-helix transcription factor family**. *The Plant Cell* 2003, **15**(8):1749-1770.
22. Zarka DG, Vogel JT, Cook D, Thomashow MF: **Cold induction of Arabidopsis *CBF* genes involves multiple ICE (inducer of *CBF* expression) promoter elements and a cold-regulatory circuit that is desensitized by low temperature**. *Plant Physiology* 2003, **133**(2):910-918.
23. Chen Y, Jiang J, Song A, Chen S, Shan H, Luo H, Gu C, Sun J, Zhu L, Fang W: **Ambient temperature enhanced freezing tolerance of *Chrysanthemum dichrum CdICE1* Arabidopsis via miR398**. *BMC biology* 2013, **11**(1):121.
24. Huang XS, Zhang Q, Zhu D, Fu X, Wang M, Zhang Q, Moriguchi T, Liu JH: ***ICE1* of *Poncirus trifoliata* functions in cold tolerance by modulating polyamine levels through interacting with arginine decarboxylase**. *Journal of experimental botany* 2015, **66**(11):3259-3274.
25. Yin X, Wang Q, Chen Q, Xiang N, Yang Y, Yang Y: **Genome-Wide Identification and Functional Analysis of the Calcineurin B-like Protein and Calcineurin B-like Protein-Interacting Protein Kinase Gene Families in Turnip (*Brassica rapa* var. *rapa*)**. *Front Plant Sci* 2017, **8**:1191.
26. Zheng Y, Luo L, Liu Y, Yang Y, Wang C, Kong X, Yang Y: **Effect of vernalization on tuberization and flowering in the Tibetan turnip is associated with changes in the expression of *FLC* homologues**. *Plant Divers* 2018, **40**(2):50-56.
27. Hayashi T, Yamaguchi T, Nakayama K, Koike S: **Effects of high nitrogen supply on the susceptibility to coolness at the young microspore stage in rice (*Oryza sativa L.*): Gene expression analysis in mature anthers**. *Plant production science* 2009, **12**(3):271-277.
28. Shi H, Chan Z: **Improvement of plant abiotic stress tolerance through modulation of the polyamine pathway**. *Journal of Integrative Plant Biology* 2014, **56**(2):114-121.
29. Song Y, Diao Q, Qi H: **Putrescine enhances chilling tolerance of tomato (*Lycopersicon esculentum Mill.*) through modulating antioxidant systems**. *Acta physiologiae plantarum* 2014, **36**(11):3013-3027.
30. Benina M, Obata T, Mehterov N, Ivanov I, Petrov V, Toneva V, Fernie AR, Gechev TS: **Comparative metabolic profiling of *Haberlea rhodopensis*, *Thellungiella halophyla*, and *Arabidopsis thaliana* exposed to low temperature**. *Front Plant Sci* 2013, **4**:499.

31. Alcázar R, Planas J, Saxena T, Zarza X, Bortolotti C, Cuevas J, Bitrián M, Tiburcio AF, Altabella T: **Putrescine accumulation confers drought tolerance in transgenic Arabidopsis plants over-expressing the homologous *Arginine decarboxylase 2 gene***. *Plant Physiology and Biochemistry* 2010, **48**(7):547-552.
32. Alcázar R, García-Martínez JL, Cuevas JC, Tiburcio AF, Altabella T: **Overexpression of *ADC2* in Arabidopsis induces dwarfism and late-flowering through GA deficiency**. *The Plant Journal* 2005, **43**(3):425-436.
33. Hummel I, Bourdais G, Gouesbet G, Couée I, Malmberg RL, El Amrani A: **Differential gene expression of arginine decarboxylase *ADC1* and *ADC2* in *Arabidopsis thaliana*: characterization of transcriptional regulation during seed germination and seedling development**. *New phytologist* 2004, **163**(3):519-531.
34. El Amrani A, Couée I, Berthomé R, Ramel F, Gouesbet G, Sulmon C: **Involvement of polyamines in sucrose-induced tolerance to atrazine-mediated chemical stress in *Arabidopsis thaliana***. *Journal of plant physiology* 2019, **238**:1-11.
35. Podlešáková K, Ugena L, Spíchal L, Doležal K, De Diego N: **Phytohormones and polyamines regulate plant stress responses by altering GABA pathway**. *New biotechnology* 2019, **48**:53-65.
36. Miura K, Ohta M, Nakazawa M, Ono M, Hasegawa PM: **ICE1 Ser403 is necessary for protein stabilization and regulation of cold signaling and tolerance**. *Plant J* 2011, **67**(2):269-279.
37. Ding Y, Li H, Zhang X, Xie Q, Gong Z, Yang S: **OST1 kinase modulates freezing tolerance by enhancing ICE1 stability in Arabidopsis**. *Dev Cell* 2015, **32**(3):278-289.
38. Kim SY, Kim SG, Kim YS, Seo PJ, Bae M, Yoon HK, Park CM: **Exploring membrane-associated *NAC* transcription factors in *Arabidopsis*: implications for membrane biology in genome regulation**. *Nucleic Acids Res* 2007, **35**(1):203-213.
39. Yang ZT, Wang MJ, Sun L, Lu SJ, Bi DL, Sun L, Song ZT, Zhang SS, Zhou SF, Liu JX: **The membrane-associated transcription factor *NAC089* controls ER-stress-induced programmed cell death in plants**. *PLoS Genet* 2014, **10**(3):e1004243.
40. Dong C-H, Agarwal M, Zhang Y, Xie Q, Zhu J-K: **The negative regulator of plant cold responses, HOS1, is a RING E3 ligase that mediates the ubiquitination and degradation of ICE1**. *Proceedings of the National Academy of Sciences of the United States of America* 2006, **103**(21):8281-8286.
41. Shi Y, Ding Y, Yang S: **Cold signal transduction and its interplay with phytohormones during cold acclimation**. *Plant and Cell Physiology* 2014, **56**(1):7-15.
42. Zhao C, Wang P, Si T, Hsu C-C, Wang L, Zayed O, Yu Z, Zhu Y, Dong J, Tao WA: **MAP kinase cascades regulate the cold response by modulating ICE1 protein stability**. *Developmental cell* 2017, **43**(5):618-629.
43. Dionisio-Sese ML, Tobita S: **Antioxidant responses of rice seedlings to salinity stress**. *Plant Science* 1998, **135**(1):1-9.
44. Wang Y, Song F, Zhu J, Zhang S, Yang Y, Chen T, Tang B, Dong L, Ding N, Zhang Q: **GSA: genome sequence archive**. *Genomics, proteomics & bioinformatics* 2017, **15**(1):14-18.

45. Lin K, Zhang N, Severing EI, Nijveen H, Cheng F, Visser RG, Wang X, de Ridder D, Bonnema G: **Beyond genomic variation-comparison and functional annotation of three Brassica rapa genomes: a turnip, a rapid cycling and a Chinese cabbage**. *Bmc Genomics* 2014, **15**(1):250.
46. Trapnell C, Roberts A, Goff L, Pertea G, Kim D, Kelley DR, Pimentel H, Salzberg SL, Rinn JL, Pachter L: **Differential gene and transcript expression analysis of RNA-seq experiments with TopHat and Cufflinks**. *Nature protocols* 2012, **7**(3):562.
47. Love MI, Huber W, Anders S: **Moderated estimation of fold change and dispersion for RNA-seq data with DESeq2**. *Genome biology* 2014, **15**(12):550.
48. Basu A, Joshi RK, Jha S: **Genetic transformation of Plumbago zeylanica with *Agrobacterium rhizogenes* strain LBA 9402 and characterization of transformed root lines**. *Plant Tissue Culture and Biotechnology* 2015, **25**(1):21-35.
49. Bowler C, Benvenuto G, Laflamme P, Molino D, Probst AV, Tariq M, Paszkowski J: **Chromatin techniques for plant cells**. *The Plant Journal* 2004, **39**(5):776-789.

Supplementary Files Legend

Fig. S1 The decision of power value. a, the horizontal axis represents different power values. b, the average network connectivity under different power values. c, network heatmap, the gene expression profile of the entire module.

Fig. S2 Correlation analysis of DEGs among samples.

Fig. S3 FPKM distribution for all samples.

Fig. S4 Number of differentially expressed genes (DEGs).

Fig. S5 Different trend analysis of DEGs and were statistically grouped into 6 subclusters.

Fig. S6 KEGG pathway analysis of module ‘Turquoise’ genes. The red box represented for the enrichment of ‘Arginine and proline metabolism’ pathway including 6 genes.

Fig. S7 Amino acid sequence alignment of AtICE1 and BrrICE1.1. The single bold line below the sequence indicated the basic region. Double lines represented the helix regions, which were connected by a loop, indicated by the dotted line.

Table S1. The primers used in this study.

Table S2. The statistics of RNA-Seq data.

Table S3. Summary statistics of map to reference genome database.

Table S4. Annotated number of DEGs.

Table S5. Promoter sequence of *BrrADC1*, *BrrADC2.1*, *BrrAlH1.1*, *BrrAlH1.2*, *BrrSAMDC1.1*, *BrrSPD2.1*.

Figures

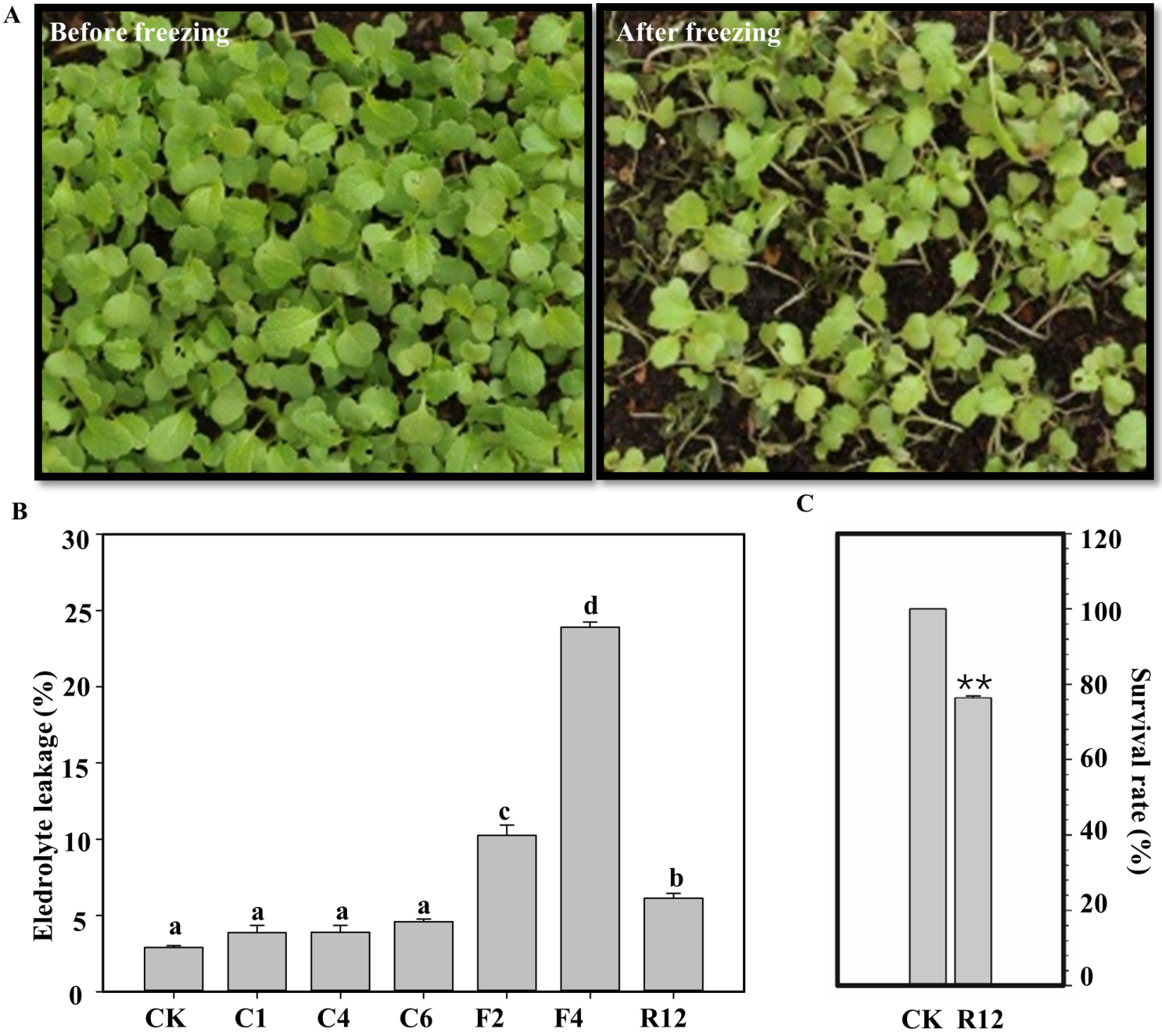

Figure 1

Freezing treatment and physiological index determination of turnip KTRG-B49. (A) Freezing phenotypes. (B) Electrolyte leakage (%). Values are the mean of 5-8 biological replicates. Bars indicate SD. Different symbols indicate significant differences between treatments ($P < 0.05$) according to Tukey's test. CK, C1, C4, C6, F2, F4, and R12 represent the samples from the untreated control; 4 °C at 1 h, 3 h, and 6 h; -2 °C at

2 h; -4 °C 1 h; and recovery for 12 h, respectively. (C) Survival rates. Asterisks indicate statistically significant differences (*P < 0.05, **P < 0.01, Student's t test).

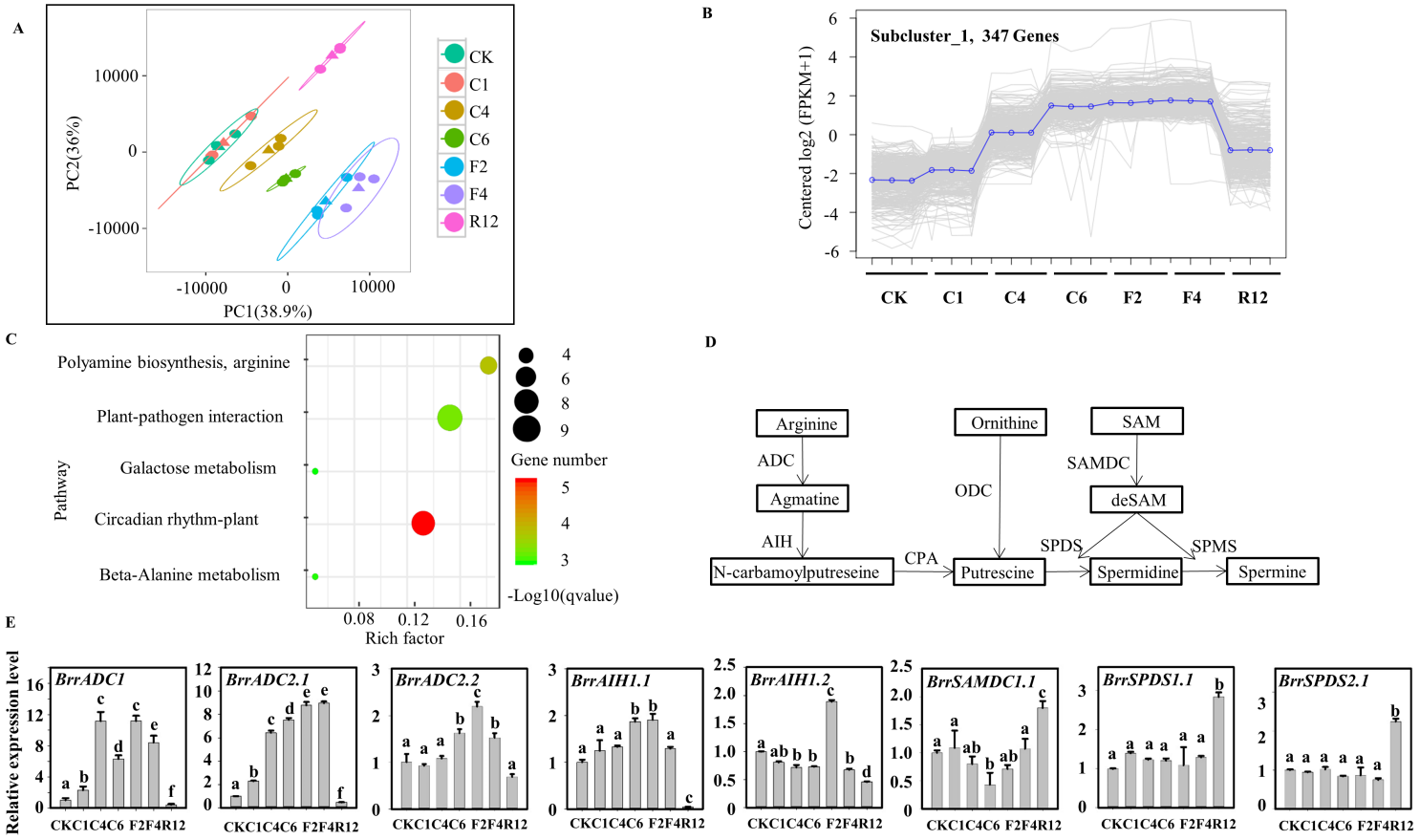

Figure 2

Transcriptome and qRT-PCR analysis of key genes involved in the polyamine biosynthesis pathway in turnip. (A) Principal component analysis (PCA) of transcriptome data. The scale of the axis is the relative distance. Different colors or shapes represent different groups of samples under freezing treatments. (B) Different trend (subcluster_1) analysis of DEGs. (C) Scatterplot of KEGG pathways enriched for differentially expressed genes (DEGs) in subcluster_1. The top 5 enriched pathway terms in the KEGG database are listed. (D) Polyamine biosynthetic pathway (right) in plants. (E) qPCR analysis of key genes involved in polyamines biosynthesis. Relative expression levels of target genes were calculated with the formula 2-ΔΔCt. Data were analyzed by one-way ANOVA according to Tukey's test. Values reflect the mean ± SD of three replicates. Means denoted by different letters were significantly different (P < 0.05). CK, C1, C4, C6, F2, F4, and R12 represent the samples from the untreated control; 4 °C at 1 h, 3 h, and 6 h; -2 °C at 2 h; -4 °C 1 h; and recovery for 12 h, respectively.

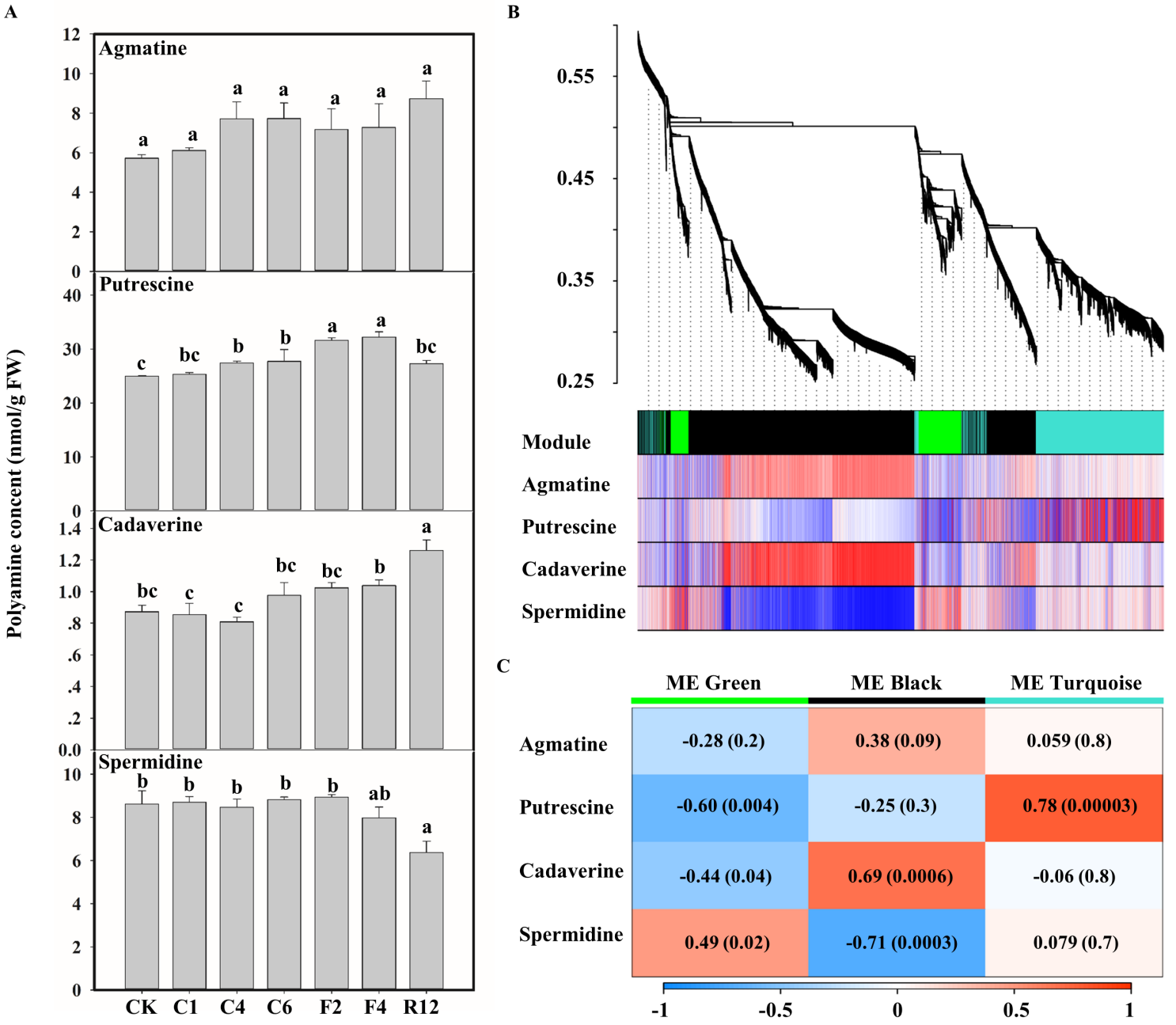

Figure 3

Determination of polyamine content after freezing treatments and weighted gene coexpression network analysis (WGCNA) analysis of module eigengenes and polyamine metabolic profiles. (A) The contents of agmatine, putrescine, cadaverine, and spermidine under freezing treatment in turnip. Values are the mean of five biological replicates. Bars indicate SD. Different symbols indicate significant differences between treatments ($P < 0.05$) according to Tukey's test. (B) Clustering dendrogram of expressed genes. Gene modules were identified by dynamic hierarchical tree cut and shown in different colors. (C) For each module, the heatmap showed module eigengene (ME) correlations to traits. Numbers in each rectangular indicate the correlation coefficients and Student's asymptotic P value (parentheses) for significant ME-trait relationships. The scale bar, bottom, indicates the range of possible correlations from positive (red, 1) to negative (blue, -1).

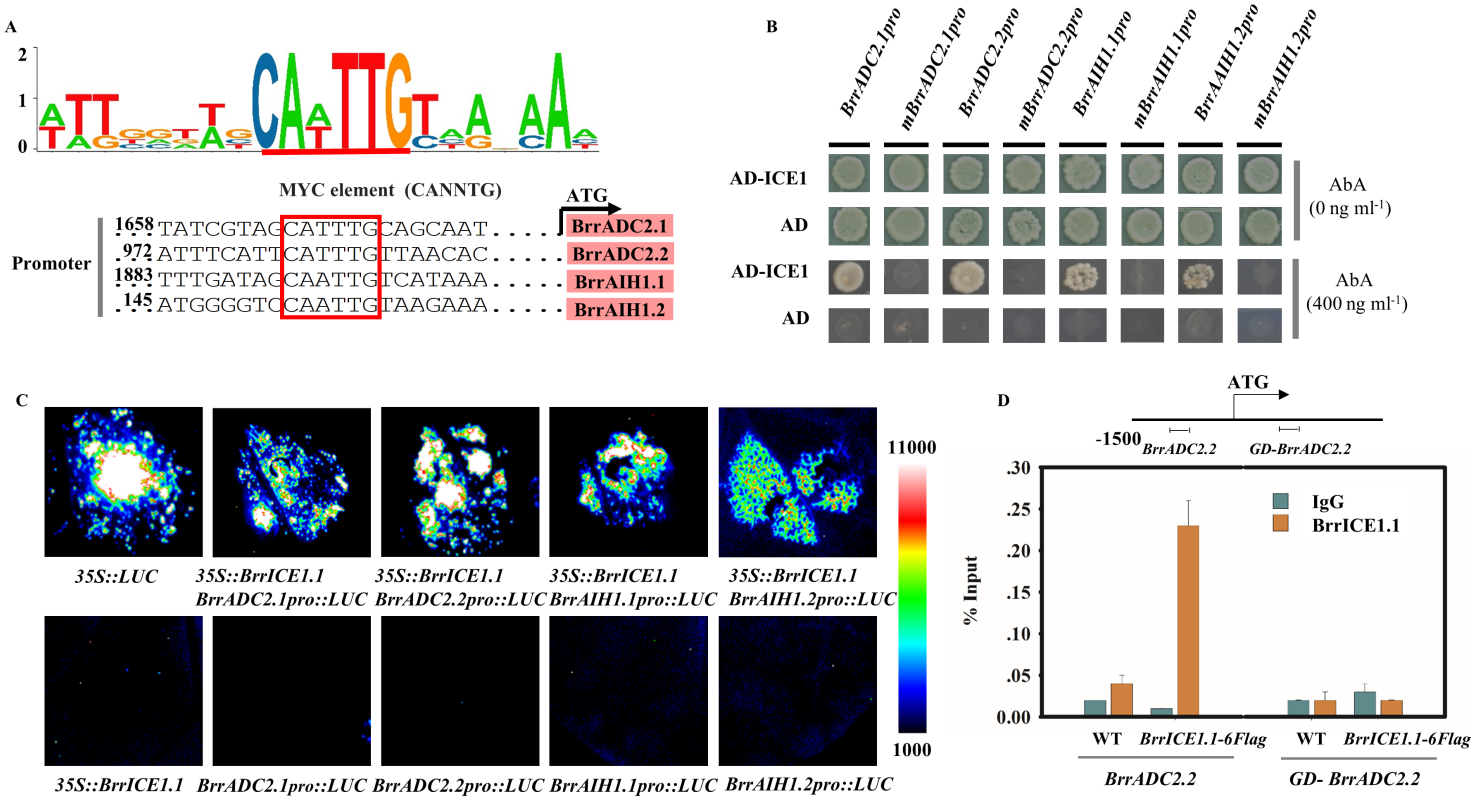

Figure 4

Binding motif analysis in the target regions of turnip BrrICE1.1 and interaction analysis of BrrICE1.1 with the promoter of the differentially expressed genes in the polyamine pathway in vivo and in vitro. (A) The potential MYC-binding site (CANNTG) of BrrICE1.1. The binding sequences of the BrrICE1.1 with BrrAIH1.1, BrrAIH1.2, BrrADC2.1, and BrrADC2.2 protein loci are shown in red. (B) Yeast one-hybrid assays showed that the MYC element mediates BrrICE1.1 binding to the BrrAIH1.1, BrrAIH1.2, BrrADC2.1, and BrrADC2.2 promoters, and the BrrAIH1.1, BrrAIH1.2, BrrADC2.1, and BrrADC2.2 promoters were mutated (deleted MYC element) to abolish the MYC element alone. The experiments were repeated three times with the same results. (C) BrrICE1.1 activated the activity of BrrAIH1.1, BrrAIH1.2, BrrADC2.1, and BrrADC2.2 in vivo. N. benthamiana leaves. Representative images of N. benthamiana leaves 72 h after infiltration are shown. (D) ChIP experiment using BrrICE1.1-6flag transgenic hair root. The structure of the BrrADC2.2 gene promoter. The primer sequence regions used for ChIP assays are marked with a horizontal line to the left of the TSS. The control primer sequence (GD) was on the left side of TSS. ChIP-qPCR showing binding of BrrICE1.1 to BrrADC2.2 promoters in vivo. WT and BrrADC2.2-GD were used as negative controls. The data are the mean of three replicates ± SD, and the asterisks indicate significant differences compared with IgG (*P < 0.05, **P < 0.01, Student's t test).

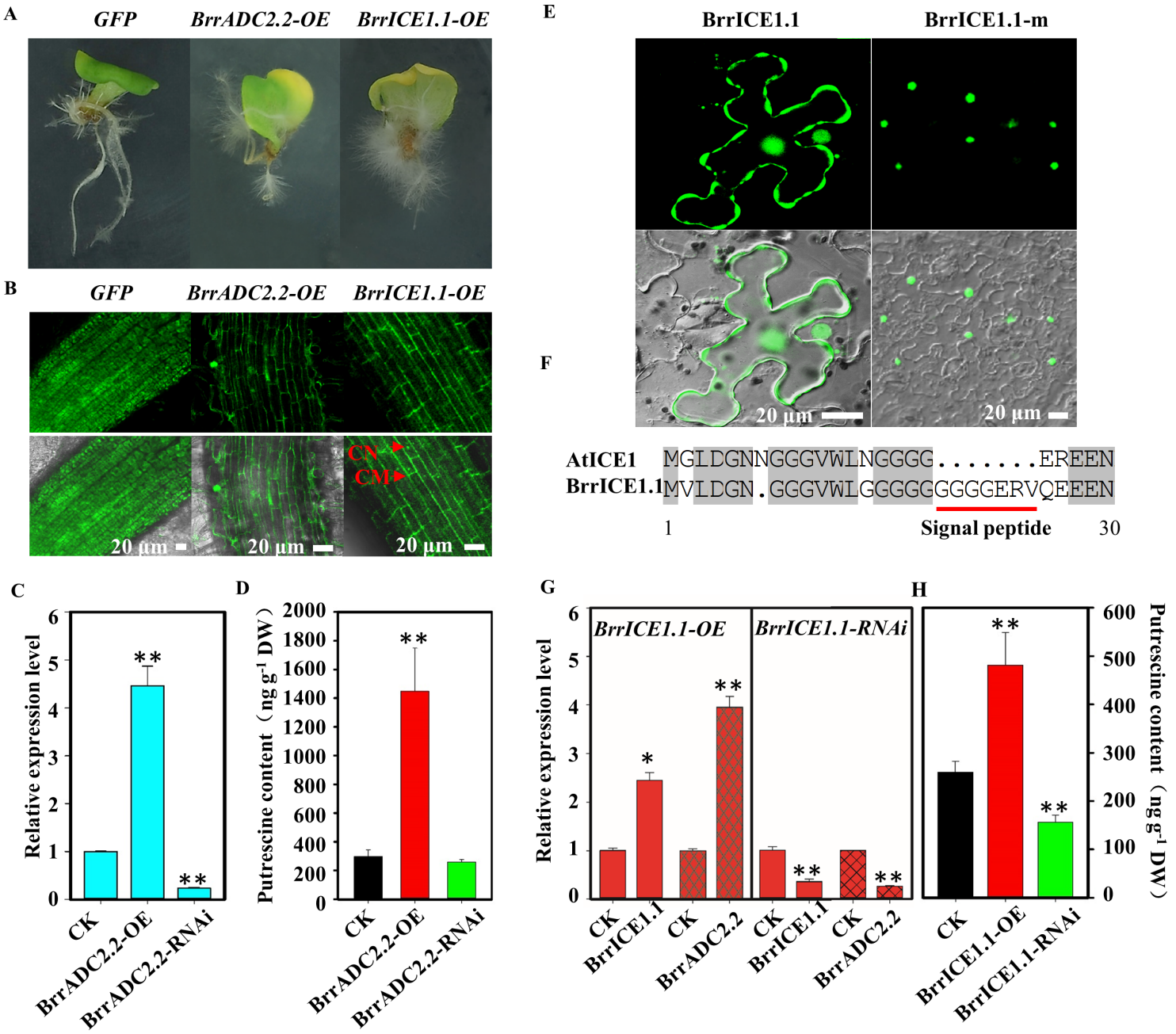

Figure 5

Detection of expression and putrescine contents in transgenic and RNAi hairy roots. (A) The phenotype of the hair root. GFP: control, BrrADC2.2-OE: overexpression of BrrADC2.2 in hair root, BrrICE1.1-OE: overexpression of BrrICE1.1 in hair root. (B) Laser confocal detection of overexpressed GFP, BrrADC2.2-OE and BrrICE1.1-OE protein in the hairy roots. CN: cell nucleus, CM: cell membrane. Bar = 20 μm. (C) (D) The expression levels of BrrADC2.2 and putrescine contents in BrrADC2.2-OE transgenic and BrrADC2.2-RNAi hairy roots compared with those of the CK. (E) Laser confocal detection of overexpressed BrrICE1.1 and its single peptide mutant (BrrICE1.1-m) protein localization in N. benthamiana leaves. Bar = 20 μm. (F) The structure of the AtICE1 and BrrICE1.1 protein at the N-terminus (1-30). The red line represents a single peptide in the BrrICE1.1 protein. (G) The expression levels of BrrICE1.1 and BrrADC2.2 in BrrICE1.1-OE

transgenic hair roots (left) and BrrICE1.1 and BrrADC2.2 in BrrICE1.1-RNAi transgenic hair roots (right). (H) Putrescine contents in BrrICE1.1-OE transgenic and BrrICE1.1-RNAi hairy roots. In (C, D, G and H), the data are the mean of three replicates ± SD, and the asterisks indicate significant differences compared with the CK (*P < 0.05, **P < 0.01, Student's t test).

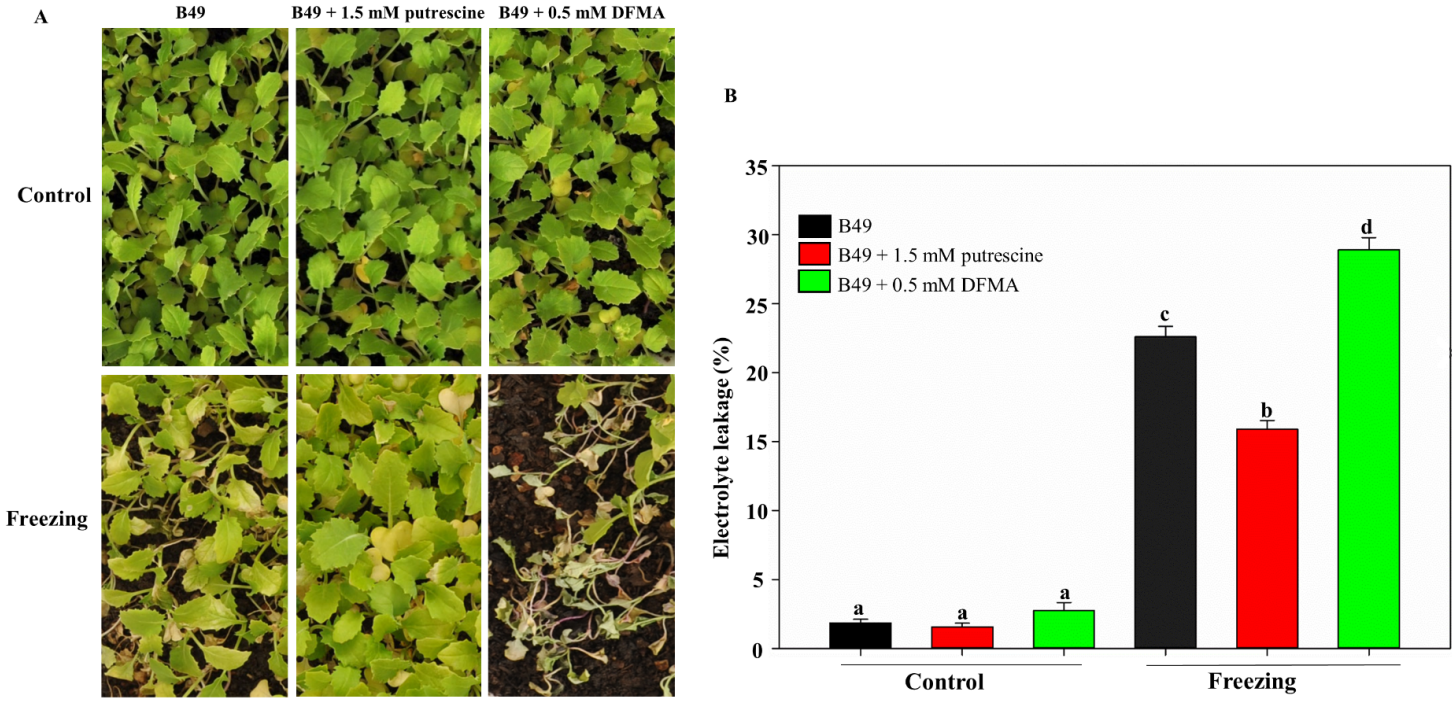

Figure 6

Effects of exogenous putrescine and its inhibitor on freezing tolerance of KTRG-B49. (A). Representative plants of B49 with and without 1.5 mM putrescine and 0.5mM DFMA before (Control) and after freezing treatment (Freezing), respectively. (B) Electrolyte leakage of leaves from control and freezing treated plants. Values are means of 5–8 biological replicates. Bars indicate SD. Different symbols indicate significant differences between treatments (P < 0.05) according to Tukey's test.

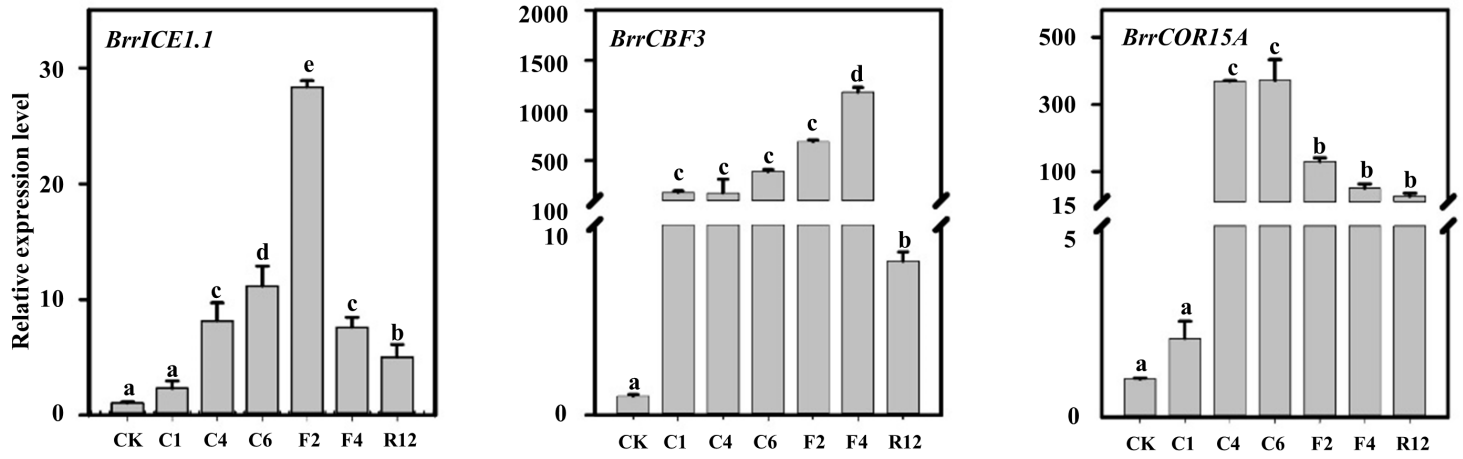

Figure 7

Expression of the BrrICE1.1, BrrCBF3 and BrrCOR15A genes upon freezing treatment with three biological and technical replicates. Different symbols indicate significant differences between treatments (P < 0.05) according to Tukey's test.

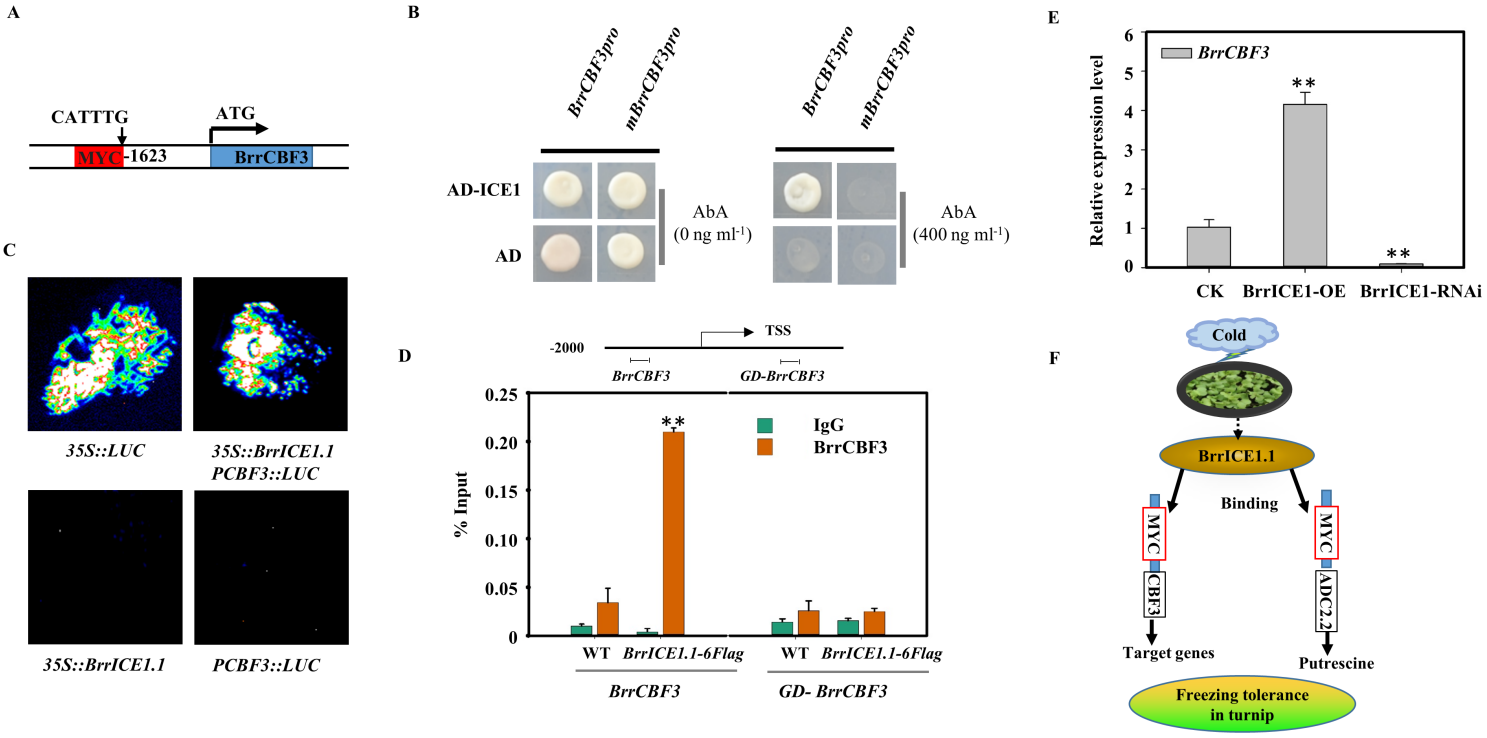

Figure 8

BrrICE1.1 bound to the BrrCBF3 promoter. (A) The potential binding site of BrrICE1.1 is the MYC element (CATTTG) in the BrrCBF3 promoter. (B) Yeast one-hybrid assays showed that the MYC element mediates BrrICE1.1 binding to the BrrCBF3 promoter and that the BrrCBF3 promoters were mutated (deleted MYC element) to abolish the MYC element alone. The experiments were repeated three times with the same results. (C) BrrICE1.1 activated the binding activity of BrrCBF3 in vivo; N. benthamiana leaves were transformed with the positive control (35S::LUC) and negative control (35S::BrrICE1.1, PCBF3::LUC), and the interaction was detected. Representative images of N. benthamiana leaves 72 h after infiltration are shown. (D) ChIP experiment using BrrICE1.1-6flag transgenic hair root. The structure of the BrrCBF3 gene promoter. The primer sequence regions used for ChIP assays are marked with a horizontal line to the left of the TSS. The control primer sequence (GD) is on the left side of the TSS. ChIP-qPCR showing binding of BrrICE1.1 to the BrrCBF3 promoters in vivo. WT and BrrCBF3-GD were used as negative controls. (E) The expression of BrrCBF3 in BrrICE1.1-OE and BrrICE1.1-RNAi transgenic hair roots. (F) BrrICE1.1 regulatory network under freezing stress in turnip. In (D) and (E), the data are the mean of three replicates ± SD, and the asterisks indicate significant differences compared with the control (*P < 0.05, **P < 0.01, Student's t test).

Supplementary Files

This is a list of supplementary files associated with this preprint. Click to download.

- Supplementaryinformation.docx